ELSEVIER

Composite Structures 50 (2000) 29–35

COMPOSITE STRUCTURES

www.elsevier.com/locate/compstruct

Three-dimensional elasticity solution for buckling of composite laminates

Haozhong Gu *, Aditi Chattopadhyay

Department of Mechanical and Aerospace Engineering, Arizona State University, Tempe, AZ 85287-6106, USA

Abstract

Three-dimensional elasticity solutions are presented for the buckling of simply supported orthotropic and laminated composite plates. A uniform prebuckling stress assumption is made for composite laminates, which is equivalent to the membrane assumption used in plate theories. The closed-form expressions for the displacements and stresses are derived and a nonlinear eigenvalue problem is constructed which is used to solve for the critical load. The results obtained from the elasticity solution are compared with the critical loads furnished by the classical laminate theory and the refined third-order shear deformation theory. The solution provides a means of accurate assessment of existing two-dimensional plate theories. © 2000 Elsevier Science Ltd. All rights reserved.

Keywords: Buckling; Composite; Three-dimensional elasticity solution

1. Introduction

The analysis of composite laminates is complicated by the presence of inherent anisotropy in material and inherent inhomogeneity among the different layers. The anisotropy and inhomogeneity lead to considerable warping of the normal to the middle surface of a composite laminates causing abrupt variations of stresses at the interfaces of the laminate. A significant amount of research has been performed to address these issues. This includes two-dimensional approximate theories such as classical laminate theory, first-order theory [10] and various higher-order theories [10,11].

Among the characteristics of these two-dimensional theories, which limit their generality in the description of laminate response, are the approximation of inplane displacements through the thickness, particularly for laminates in which the stiffness properties vary dramatically from layer to layer. Other important limiting factors are the presence of boundary conditions in the plate theories that precludes the precise calculation of boundary layer effects, such as stress concentration factors and the approximation of shear deformation, implied by the hypothesis of plate theories. Finally the assumption of a state of plane stress in the constitutive relations eliminates the possibility of rigorous calculation of interlaminar stresses. The development of elasticity solutions is therefore necessary to assess the validity of these approximate theories.

An elasticity solution was derived by Pagano [3,5,6] for the bending problem of composite laminates. Recently, two-dimensional elasticity solutions for the buckling of simply supported composite plates, whose behavior are referred to as cylindrical bending, was developed by Chattopadhyay and Gu [2]. The solutions were used to investigate the limitations of approximate two-dimensional theories, based on either the classical Kirchhoff–Love hypothesis or the refined displacement field. However, for cases where the plate deformation is not restricted to cylindrical bending, rigorous three-dimensional analytical solutions based on the exact theory of elasticity should be obtained.

Three-dimensional elasticity solutions are only available for composite plates subjected to a transverse load distribution. Pagano [4] first derived an elasticity solution for rectangular bidirectional two and three layered composites and sandwich plates. This study was later extended to address multilayered composites by Pagano and Hatfield [7]. Noor and Burton [9] conducted the assessment of shear deformation theory for multilayered composite plates by using simplified discrete-layer theories and obtained the solution for antisymmetrically laminated anisotropic plates in their later research [8]. However, no effort has been reported in developing a three-dimensional solution, based on the theory of elasticity, to address the buckling of composite plates.

* Corresponding author.

PII: S0263-8223(00)00066-0

In this paper, an exact solution, based on the three-dimensional elasticity theory, is presented for buckling of simply supported orthotropic plates and laminated composite plates. Numerical results are presented for unidirectional layered composite plates and multi-layer laminated plates subject to axial compressive load. These results are then compared with those obtained using classical laminate theory and other improved laminate theories. The developed theory therefore serves as a tool for assessing the accuracy of the existing laminate theories for composites with moderately thick and thick constructions.

2. Development of buckling equations

For a three-dimensional elastic body (Fig. 1), the equations of equilibrium are written in terms of the stress tensor Σ and the deformation gradient $\mathbf{F}$ as follows.

$$\operatorname{div}(\Sigma \cdot \mathbf{F}^{\mathrm{T}}) = 0, \tag{1}$$

where the deformation gradient $\mathbf{F}$ can be expressed by the derivatives of the displacements u, v and w.

$$\mathbf{F} = \begin{bmatrix} 1+u_{,x} & u_{,y} & u_{,z} \\ v_{,x} & 1+v_{,y} & v_{,z} \\ w_{,x} & w_{,y} & 1+w_{,z} \end{bmatrix}, \tag{2}$$

where the comma denotes partial differentiation with respect to the index that follows.

The membrane primary prebuckling state of orthotropic plates whose material axes are parallel to the geometric axes can be truly simulated by

$$\sigma_x^0 = -p, \quad \sigma_y^0 = \sigma_z^0 = \tau_{yz}^0 = \tau_{xz}^0 = \tau_{xy}^0 = 0. \tag{3}$$

For an orthotropic layer, the exact constitutive equations can be stated as follows.

$$\begin{bmatrix} \sigma_x \\ \sigma_y \\ \sigma_z \\ \tau_{yz} \\ \tau_{xz} \\ \tau_{xy} \end{bmatrix} = \begin{bmatrix} C_{11} & C_{12} & C_{13} & 0 & 0 & 0 \\ C_{12} & C_{22} & C_{23} & 0 & 0 & 0 \\ C_{13} & C_{23} & C_{33} & 0 & 0 & 0 \\ 0 & 0 & 0 & C_{44} & 0 & 0 \\ 0 & 0 & 0 & 0 & C_{55} & 0 \\ 0 & 0 & 0 & 0 & 0 & C_{66} \end{bmatrix} \begin{bmatrix} u_{,x} \\ v_{,y} \\ w_{,z} \\ v_{,z}+w_{,y} \\ u_{,z}+w_{,x} \\ u_{,y}+v_{,x} \end{bmatrix} \tag{4}$$

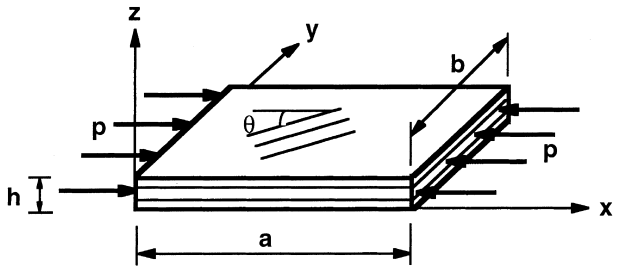

Fig. 1. Geometry of the composite plate.

in which C_{ij}, $(i,j=1,3)$ denote the reduced stiffness coefficients. The displacements for the prebuckling state are derived as follows:

$$\begin{aligned} &u_{,x}^0 = -\frac{C_{22}C_{33}-C_{23}^2}{\Delta}p, \quad v_{,x}^0 = \frac{C_{12}C_{33}-C_{13}C_{23}}{\Delta}p, \\ &w_{,z}^0 = \frac{C_{13}C_{22}-C_{12}C_{23}}{\Delta}p, \\ &u_{,y}^0 = u_{,z}^0 = v_{,x}^0 = u_{,z}^0 = w_{,x}^0 = w_{,y}^0 = 0, \\ &\Delta = C_{11}C_{22}C_{33} + 2C_{12}C_{13}C_{23} - C_{33}C_{12}^2 - C_{22}C_{13}^2 - C_{11}C_{23}^2. \end{aligned} \tag{5}$$

At the critical load, there are two possible infinitely close positions of equilibrium. Using superscript $(\,)^0$ to denote the components of the stresses and the displacements corresponding to the primary position, a perturbed position is defined as follows.

$$\begin{aligned} &\sigma_x = \sigma_x^0 + \alpha\sigma_x^1, \quad \sigma_y = \sigma_y^0 + \alpha\sigma_y^1, \quad \sigma_z = \sigma_z^0 + \alpha\sigma_z^1, \\ &\tau_{xz} = \tau_{xz}^0 + \alpha\tau_{xz}^1, \quad \tau_{yz} = \tau_{yz}^0 + \alpha\tau_{yz}^1, \quad \tau_{xy} = \tau_{xy}^0 + \alpha\tau_{xy}^1, \\ &u = u^0 + \alpha u^1, \quad v = v^0 + \alpha v^1, \quad w = w^0 + \alpha w^1, \end{aligned} \tag{6}$$

where σ_i and τ_{ij} $(i,j=x,y,z)$ are the stress components, α is an infinitesimally small quantity and $\alpha(\,)^1$ denote the increments in stresses or displacements necessary to shift from the initial position of equilibrium to the new equilibrium position. Using the prebuckling solution (Eqs. (3) and (5)) and the perturbation condition (Eq. (6)), the buckling equations are obtained by collecting the α terms.

$$\begin{aligned} &[\sigma_x(1+u_{,x}^0) - pu_{,x}]_{,x} + [\tau_{xy}(1+u_{,x}^0)]_{,y} \\ &\quad + [\tau_{xz}(1+u_{,x}^0)]_{,z} = 0, \\ &[\tau_{xy}(1+v_{,y}^0) - pv_{,x}]_{,x} + [\sigma_y(1+v_{,y}^0)]_{,y} \\ &\quad + [\tau_{yz}(1+v_{,y}^0)]_{,z} = 0, \\ &[\tau_{xz}(1+w_{,z}^0) - pw_{,x}]_{,x} + [\tau_{yz}(1+w_{,y}^0)]_{,y} \\ &\quad + [\sigma_z(1+w_{,z}^0)]_{,z} = 0, \end{aligned} \tag{7}$$

where the superscript $(\,)^1$ is omitted for the convenience of notation. Inserting the constitutive relation (Eq. (4)) into Eq. (7), the above buckling equation can be expressed in terms of displacements as follows.

$$\begin{aligned} &\left(C_{11} - \frac{p\Delta}{\Delta - C_{22}C_{33} + C_{23}^2}\right)u_{,xx} + C_{66}u_{,yy} + C_{55}u_{,zz} \\ &\quad + (C_{12}+C_{66})v_{,xy} + (C_{13}+C_{55})w_{,xz} = 0, \\ &(C_{12}+C_{66})u_{,xy} + \left(C_{66} - \frac{p\Delta}{\Delta + C_{12}C_{33} - C_{13}C_{23}}\right)v_{,xx} \\ &\quad + C_{22}v_{,yy} + C_{44}v_{,zz} + (C_{23}+C_{44})w_{,yz} = 0, \\ &(C_{13}+C_{55})u_{,xy} + (C_{23}+C_{44})v_{,yz} \\ &\quad + \left(C_{55} - \frac{p\Delta}{\Delta + C_{22}C_{13} - C_{12}C_{23}}\right)w_{,xx} \\ &\quad + C_{44}w_{,yy} + C_{33}w_{,zz} = 0. \end{aligned} \tag{8}$$

3. Solution of simply supported unidirectional composite plate

For the simply supported plate, the boundary conditions for the buckling state are simulated by

$$\begin{aligned}&\sigma_x = v = w = 0 \quad \text{at } x = 0,\ a,\\ &\sigma_y = u = w = 0 \quad \text{at } y = 0,\ b,\end{aligned} \tag{9}$$

where a and b are the length and the width of the plate, respectively. The solution to the boundary value problem described in Eqs. (8) and (9) can be obtained by assuming the following form for the displacements:

$$\begin{aligned}u &= U_{mn}(z)\cos\frac{m\pi x}{a}\sin\frac{n\pi y}{b},\\ v &= V_{mn}(z)\sin\frac{m\pi x}{a}\cos\frac{n\pi y}{b},\\ w &= W_{mn}(z)\sin\frac{m\pi x}{a}\sin\frac{n\pi y}{b},\end{aligned} \tag{10}$$

where $U(z)$, $V(z)$ and $W(z)$ are unknown functions of z, and m and n are the number of buckling waves along the length and the width of the plate, respectively. Assuming that

$$(U_{mn},\ V_{mn},\ W_{mn}) = (U^c_{mn},\ V^c_{mn},\ W^c_{mn})e^{\lambda z}, \tag{11}$$

where U^c_{mn}, V^c_{mn} and W^c_{mn} are unknown constants. Substituting Eqs. (10) and (11) into Eq. (8), the following set of algebraic equations are obtained:

$$\begin{aligned}&\left[C_{55}\lambda^2 - \frac{m^2\pi^2}{a^2}\left(C_{11} - \frac{p\Delta}{\Delta - C_{22}C_{33} + C_{23}^2}\right) - \frac{n^2\pi^2}{b^2}C_{66}\right]U^c_{mn}\\ &\quad + \frac{mn\pi^2}{ab}(C_{12} + C_{66})V^c_{mn} + \frac{m\pi}{a}\lambda(C_{13} + C_{55})W^c_{mn} = 0,\\ &\quad - \frac{mn\pi^2}{ab}(C_{12} + C_{66})U^c_{mn}\\ &\quad + \left[C_{44}\lambda^2 - \frac{m^2\pi^2}{a^2}\left(C_{66} - \frac{p\Delta}{\Delta + C_{12}C_{33} - C_{13}C_{23}}\right)\right.\\ &\qquad \left. - \frac{n^2\pi^2}{b^2}C_{22}\right]U^c_{mn} + \frac{n\pi}{b}\lambda(C_{23} + C_{44})W^c_{mn} = 0,\\ &\quad - \frac{m\pi}{a}\lambda(C_{13} + C_{55})U^c_{mn} - \frac{n\pi}{b}\lambda(C_{23} + C_{44})V^c_{mn}\\ &\quad + \left[C_{33}\lambda^2 - \frac{m^2\pi^2}{a^2}\left(C_{55} - \frac{p\Delta}{\Delta + C_{22}C_{13} - C_{12}C_{23}}\right)\right.\\ &\qquad \left. - \frac{n^2\pi^2}{b^2}C_{44}\right]U^c_{mn} = 0.\end{aligned} \tag{12}$$

Nontrivial solutions of this set of equation only exist if the determinant of the coefficient vanishes, which leads to the following algebraic equation in λ:

$$A\lambda^6 + B\lambda^4 + C\lambda^2 + D = 0, \tag{13}$$

where A, B, C and D are derived constants. Eq. (13) can be transformed to a third-order equation represented as

$$\gamma^3 + \mathrm{d}\gamma + f = 0, \tag{14}$$

where

$$\begin{aligned}&\gamma = \lambda^2 - \frac{B}{3A}, \quad d = -\frac{3CA + B^2}{3A^2},\\ &f = -\frac{2B^2 + 9ABC + 27DA^2}{27A^3}.\end{aligned} \tag{15}$$

Eq. (15) has three distinct real roots if

$$\frac{f^2}{4} + \frac{d^3}{27} < 0. \tag{16}$$

For fiber-reinforced composite laminates, previous numerical studies conducted by varying material properties and plate dimensions show that the inequality (16) is always satisfied [1,4]. Hence, the three real roots of Eq. (14) are given by

$$\begin{aligned}&\gamma_j = 2\left(-\frac{d}{3}\right)^{1/2}\cos\left(\frac{\phi}{3},\quad \frac{\phi + 2\pi}{3},\quad \frac{\phi + 4\pi}{3}\right),\\ &\quad j = 1, 2, 3,\end{aligned} \tag{17}$$

where

$$\cos\phi = -\frac{f\sqrt{27}}{2(-d)^{3/2}}. \tag{18}$$

Depending on the sign of the quantity $(\gamma + B/3A)$, the roots for γ can be three real or imaginary pairs. Recalling Eqs. (11), (12) and (15), the general solution for U, V and W can now be written as follows:

$$\begin{bmatrix}U_{mn}\\ V_{mn}\\ W_{mn}\end{bmatrix} = \sum_{j=1}^{3}\begin{bmatrix}F^j_{xmn} & S^j_{xmn}\\ F^j_{ymn} & S^j_{ymn}\\ F^j_{zmn} & S^j_{zmn}\end{bmatrix}\begin{bmatrix}a_jG^j_{mn}\\ b_jH^j_{mn}\end{bmatrix}, \tag{19}$$

where F^j_{imn} and S^j_{imn} $(i = x, y, z)$ are functions of the load variable p, a_j and b_j are undetermined constants and

$$\begin{aligned}&G^j_{mn} = \exp(\lambda_j z), \quad H^j_{mn} = \exp(-\lambda_j z) \quad \text{if } \gamma_j + B/3A > 0,\\ &G^j_{mn} = \cos(|\lambda_j|z), \quad H^j_{mn} = \sin(|\lambda_j|z) \quad \text{if } \gamma_j + B/3A < 0.\end{aligned} \tag{20}$$

Finally, using the stress-displacement relations (Eq. (4)) in conjunction with Eq. (19), the stress components are obtained. The remaining boundary conditions at the top and the bottom surfaces of the plate, for the buckling problem, are as follows:

$$\begin{aligned}&\sigma_z(x, 0) = \sigma_z(x, h) = 0,\\ &\tau_{xz}(x, 0) = \tau_{xz}(x, h) = 0,\\ &\tau_{yz}(x, 0) = \tau_{yz}(x, h) = 0,\end{aligned} \tag{21}$$

where h is the thickness of the plate. For a single layered plate, the six undetermined constants a_j and b_j. $(j = 1, 2, 3)$ can be determined (by the relationship) from the six boundary conditions (Eq. (21)) applied at the surface of the plate. Therefore, application of the boundary conditions (Eq. (21)) to the stress expressions lead to a system of a nonlinear eigenvalue problem with four simultaneous equations for eigenvalues p. The general

form of this nonlinear eigenvalue problem of size 6×6 is expressed as

$$\mathbf{A}(p)\mathbf{a} = 0. \tag{22}$$

where vector $\mathbf{a}$ consists of the undetermined constants a_j and b_j. Using the Taylor expansion, Eq. (22) can be written as follows

$$(\mathbf{A}_0 - p\mathbf{A}_1 - p^2\mathbf{A}_2 - \cdots - p^k\mathbf{A}_k - \cdots)\mathbf{a} = \mathbf{0}. \tag{23}$$

4. Composite laminates

For the laminated composite plate (Fig. 1), denoting h_i to be the thickness of the ith layer ($i = 1, 2, \ldots, k$, where k is the number of layers), the total plate thickness $h = \sum_{i=1}^{k} h_i$. An assumption of the uniform prebuckling stress in each layer, which is equivalent to the membrane assumption used in plate theories, is made for the composite plates. That is

$$\sigma_x^{0(i)} = -p, \quad \sigma_y^{0(i)} = \sigma_z^{0(i)} = \tau_{yz}^{0(i)} = \tau_{xz}^{0(i)} = \tau_{xy}^{0(i)} = 0, \tag{24}$$

in which the superscription (i) is an index used to identify quantities in the ith layer. The displacements for prebuckling state expressed in Eq. (5) are valid in each layer. Therefore the solution procedure for the derived boundary value problem which is described in Eqs. (8)–(22) is also valid within each layer. To establish continuity of tractions and displacements at the interfaces between layers we must satisfy the following conditions in local coordinates:

$$\begin{aligned}
&\tau_{xz}^{(i)}(x, y, h_i) = \tau_{xz}^{(i+1)}(x, y, 0),\\
&\tau_{yz}^{(i)}(x, y, h_i) = \tau_{yz}^{(i+1)}(x, y, 0),\\
&\sigma_z^{(i)}(x, y, h_i) = \sigma_z^{(i+1)}(x, y, 0),\\
&u^{(i)}(x, y, h_i) = u^{(i+1)}(x, y, 0),\\
&v^{(i)}(x, y, h_i) = v^{(i+1)}(x, y, 0),\\
&w^{(i)}(x, y, h_i) = w^{(i+1)}(x, y, 0),\\
&\quad i = 1, 2, \ldots, k-1.
\end{aligned} \tag{25}$$

Using the above continuity equations and the remaining boundary conditions expressed in Eq. (21), a set of global nonlinear eigenvalue equations of size of $6k \times 6k$ are obtained for solving the critical buckling load, p, of the laminated composite plate. The general form of this nonlinear eigenvalue problem is similar to that expressed in Eqs. (22) and (23).

5. Results and discussions

As an illustrative example, the critical load was determined for a random short-fiber composite plate with various length-to-thickness (a/h) ratios. The material properties for the composite are listed in Table 1, where L represents the direction parallel to the fibers, T the transverse direction and v_{LT} is the Poisson's ratio measuring strain in the transverse direction under axial normal stress in the L direction. In the example, L corresponds to x-direction and T corresponds to y-direction as shown in Fig. 1.

Since the material properties of the random short-fiber composite are close to properties of isotropic material, it is expected that the transverse shear effect and the transverse normal effect are very small. Fig. 2 presents the critical loads from the exact elasticity solution, which are normalized with respect to the value obtained using the classical laminate theory (CLT), and are compared with those obtained using the classical laminate theory and the refined third-order theory of [10], for a wide range of a/h ratios. Although the three solutions merge for sufficiently thin plates, CLT exhibits a significant deviation from the other theories as shown in Fig. 2. For $a/h = 5$, the critical buckling load predicted by the exact elasticity solution is only about seventy eight percent of the value predicted by CLT. However, the results of the refined third-order theory show a good agreement with those obtained using the exact elasticity solution over a wide range of the length-to-thickness ratios. The maximum deviation is only about two percent between the value predicted by the refined third-order theory and the exact elasticity solution for very thick plates ($a/h = 3$–13).

Next, results are obtained for unidirectional graphite/epoxy (Type 1) composite laminates and are compared with those obtained using the two-dimensional theories mentioned above. The results of the normalized critical load are presented in Figs. 3 and 4 for a range of length-to-thickness ratios varying from thin to thick. In an extreme case where the plate is thin enough, all results converge to the same solution. As seen from Fig. 4, at lower values of a/h, deviations are observed from CLT. However, once again, the refined third-order theory shows good agreement with the exact elasticity solution for thin and moderately thick laminates. For thick laminates ($a/h < 10$), even the refined third-order theory exhibits noticeable deviation from the exact elasticity

Table 1
Material property of composites

Type of material	E_L	E_T	G_{LT}	G_{TT}	$v_{LT} = v_{TT}$
Random short-fiber	1.58	1.1	0.36	0.36	0.22
Graphite/epoxy (Type 1)	25	1	0.5	0.2	0.25
Boron/epoxy	30	2.7	0.65	0.37	0.21
Graphite/epoxy (Type 2)	20	2.1	0.85	0.85	0.21

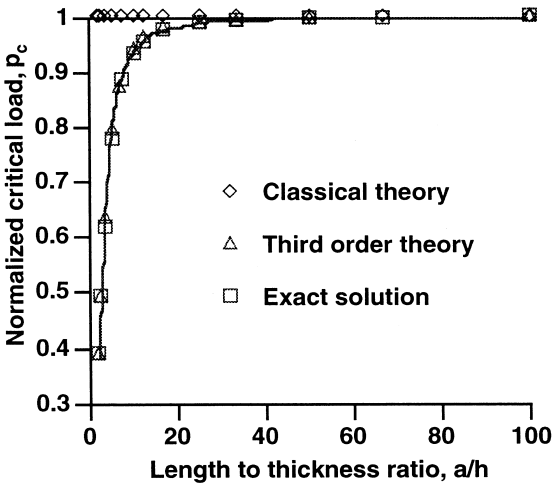

Fig. 2. Comparison of critical load for unidirectional layered random short-fiber plates.

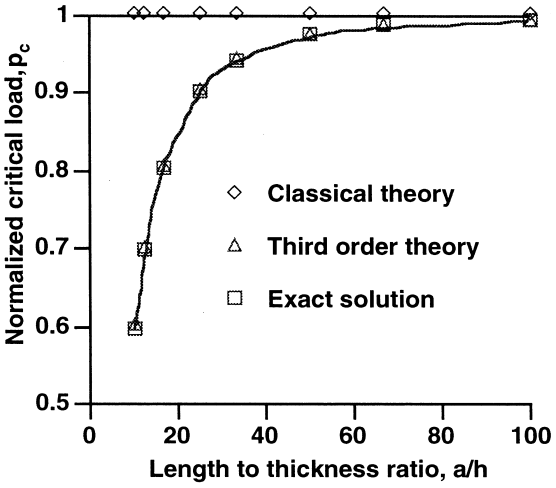

Fig. 3. Comparison of critical load for thin and moderate thick plates made of unidirectional layered graphite/epoxy (Type 1).

solution. For example, at $a/h = 5$, the critical load predicted by the refined third-order theory is 5% higher than the value obtained using the exact elasticity solution. This observation proves that the anisotropy in material lead to considerable warping of the normal to the middle surface of the plate which cause more transverse shear effects in the laminates. The higher the level of anisotropy in the material, the more significant are the effects of transverse shear on buckling behavior of laminates.

A cross-ply boron/epoxy composite laminate is also examined. The stacking sequence in this example is $[0^0/90^0/0^0]$. As shown in Figs. 5 and 6, although all results converge to the same solution in the extreme case where the plate is thin enough, significant deviations are observed in the critical load values among all three solution techniques for moderately thick and thick laminates, compared to that exhibited by the unidirectional laminates. For example, at $a/h = 5$, the critical load predicted by the refined third-order theory is 14% higher than the value obtained using the exact elasticity solution, while the critical load computed by the exact elasticity solution is only about 37% of the value computed by CLT. This phenomenon is very different from what is observed for orthotropic plates and the reason is largely due to the complexity of transverse shear and normal stress distributions in composite laminates. The anisotropy of the composite material causes considerable warping of the normal to the middle surface within the laminate and the inhomogeneity of composite laminates leads to abrupt variations of stresses at the interfaces in the laminates.

The effect of two relative stiffnesses, along geometric axis x and y, for cross-ply boron/epoxy laminates is studied. The stacking sequence is $[0^0_{n0/2}/90^0_{n90}/0^0_{n0/2}]$, in which n_0 is the number of 0° plies, n_{90} the number of

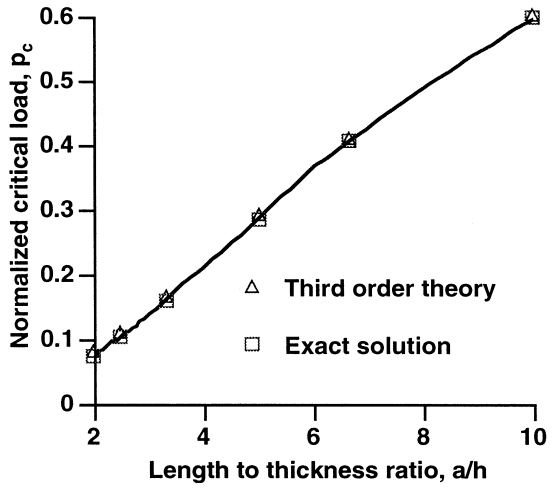

Fig. 4. Comparison of critical load for thick plates made of unidirectional layered graphite/epoxy (Type 1).

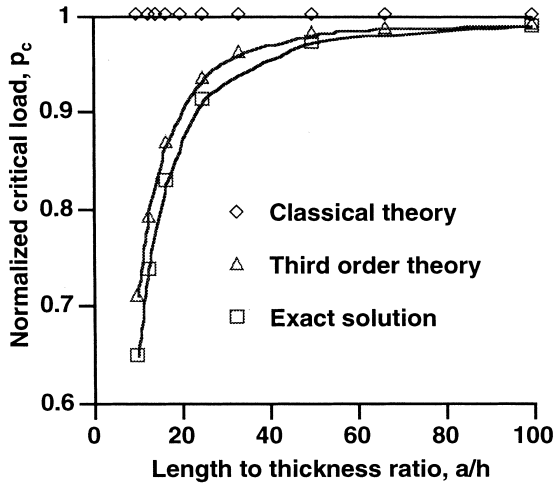

Fig. 5. Comparison of critical load for thin and moderate thick $[0^0/90^0/0^0]$ boron/epoxy plates.

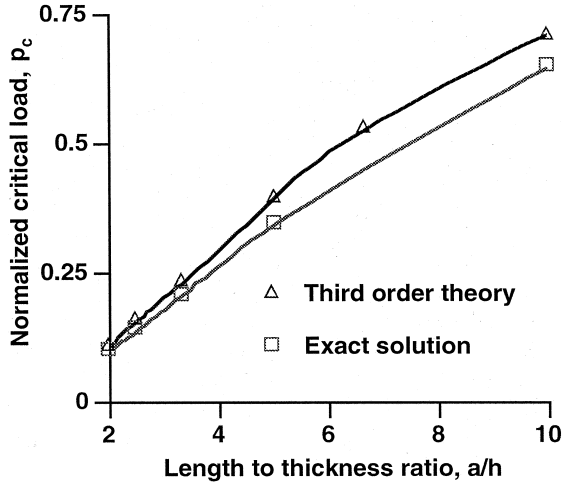

Fig. 6. Comparison of critical load for thick $[0^0/90^0/0^0]$ boron/epoxy plates.

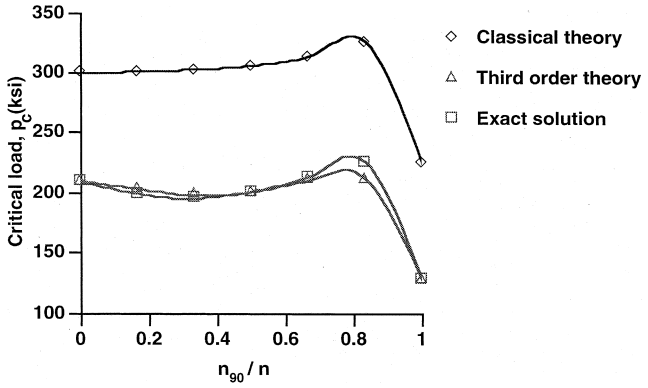

Fig. 7. Comparison of critical load by varying the number of 0° and 90° layers in $[0^0{}_{n0/2}/90^0{}_{n90}/0^0{}_{n0/2}]$ boron/epoxy plates, $n_0 + n_{90} = n$ and $a/h = 10$.

90° plies and the total number of plies used in this example is 12 ($n = n_0 + n_{90} = 12$). Fig. 7 presents the variation of the critical load with increase in the number of 90° plies. Several observations are made which are common to all three solutions. First, the critical load of laminates with unidirectional 0° plies is almost double the critical load of laminates with unidirectional 90° plies since the stiffness along the loading direction is much larger than that along the perpendicular direction. Second, the maximum critical load occurs around $n_{90}/n \approx 0.8$, at which the bending stiffnesses along the x and y direction are approximately the same. Although the CLT provides a poor prediction of the critical loads, results computed by the refined third-order theory agree quite well with those obtained using the exact elasticity solution in an overall sense. However, the results computed by refined third-order theory over predicts the critical load in the range $0 \leqslant n_{90}/n \leqslant 0.48$ and under estimates it in the range of $0.48 \leqslant n_{90}/n \leqslant 1$. The largest deviation observed here, between the refined third-order theory and the exact elasticity solution, is about 6%.

Of particular interest, for three-dimensional cases, is the variation of the critical load with changes in plate length to width ratios. The graphite/epoxy (Type 2) laminates with $[0^0_3/90^0_3]_S$ stacking sequence is used to compare the critical load, the buckling modes and the deviation in solutions of other two solutions from the exact elasticity solution (Table 2). The thickness of the laminates is 0.1 in and the area ($a \times b$, see Fig. 1) is 1 in.^{2} The critical loads computed by CLT show errors up to seventy seven percent, compared to those predicted by the exact elasticity solution. The refined third-order theory matches the exact elasticity solution very well in this case since the ratio of $n_{90}/n = 0.5$ in this example is near the transition point (Fig. 7) at which the critical loads calculated by the refined third-order theory moves from being over estimated to being under estimated. In the Table 2, (m, n) represent the buckling modes of the composite plate, in which m and n are the number of buckling waves along the length and the width, respectively. The buckling modes calculated by the refined

Table 2
Comparison of critical load from exact solution with various plate theories for $[0^0_3/90^0_3]_S$ graphite/epoxy (type 2) laminates ($a \times b = 1\text{in}^2$ and $h = 0.1$ in)

Length to width ratio, *a/b*	Critical load, p_c (ksi) (m, n), (% of difference)		
	Classical theory	Third-order theory	Exact solution
0.25	597.3	334.3	335.9
	(1, 1) (+77.8%)	(1, 1) (−0.33%)	(1, 1)
0.5	317.4	227.0	226.8
	(1, 1) (+39.9%)	(1, 1) (+0.09%)	(1, 1)
1	221.3	183.7	182.9
	(1, 1) (+20.9%)	(1, 1) (+0.44%))	(1, 1)
2	437.6	318.5	316.8
	(1, 1) (+38.1%)	(2, 1) (+0.54%)	(2, 1)
3	553.8	422.7	420.5
	(2, 1) (+31.7%)	(3, 1) (+0.52%)	(3, 1)
4	740.0	506.2	508.3
	(3, 1) (+45.6%)	(4, 1) (−0.41%)	(4, 1)

third-order theory and the exact elasticity solution are identical over a wide range of length to width ratios. Significant differences are observed between the results of the elasticity solution and CLT for $a/b > 1$. In the case of $a/b = 3$, for example, the buckling mode predicted by elasticity solution and the refined third-order theory is (3, 1), while that obtained using CLT is (2, 1). Table 2 also shows that the refined third-order theory under estimates the critical loads for laminates with smaller length to width ratio ($a/b = 0.5$) or larger length to width ratio ($a/b = 4$).

6. Conclusion

In conclusion, a three-dimensional exact elasticity solution has been presented for the buckling of simply supported composite laminates consisting of arbitrary numbers of orthotropic layers. Since the solutions are exact within the assumptions of linear elasticity, they are free from the simplifying assumptions imposed by the two-dimensional theories. Therefore there are no distinctions between thick and thin plates and both transverse shear deformation and transverse normal deformation are automatically taken into account. The following specific observations have been made.

1. The developed three-dimensional solution technique provides a framework against which comparisons can be made of classical and other two-dimensional theories. It also provides insight into the basis of assumptions that are required in the formulation of more general theories for composite laminates.
2. The results of the refined third-order theory for critical load agree well with the exact elasticity solution for critical loads and buckling modes, while solutions from CLT show poor prediction in both for thick laminates.
3. The refined third-order theory performs more poorly in the case of multi-layer laminates, compared to unidirectional laminates.
4. The laminate stiffnesses variation, along the loading and the transverse direction, affects the solution of refined third-order theory. This leads to slightly over or under estimation of critical loads, compared to the exact elasticity solution.

Acknowledgements

The research was supported by the US Army Research Office, Grant number DAAH04-93-G-0043, Technical monitor, Dr. Gary Anderson.

References

[1] Bhaskar K, Varadan TK. Exact elasticity solution for laminated anisotropic cylindrical shells. J Appl Mech 1993;41–7.
[2] Chattopadhyay A, Gu H. Exact elasticity solution for buckling of composite laminates. Compos Struct 1996;34(3):291–9.
[3] Pagano NJ. Exact solutions for composite laminates in cylindrical bending. J Compos Mater 1969;3:398–411.
[4] Pagano NJ. Exact solutions for rectangular bidirectional composites and sandwich plates. J Compos Mater 1970;4:20–35.
[5] Pagano NJ. Influence of shear coupling in cylindrical bending of anisotropic laminates. J Compos Mater 1970;4:330–43.
[6] Pagano NJ, Wang ASD. Further study of composite laminates under cylindrical bending. J Compos Mater 1971;5:521–8.
[7] Pagano NJ, Hatfield SJ. Elastic behavior of multilayered bidirectional composites. AIAA J 1972;10:931–3.
[8] Noor AK, Burton WS. Three-dimensional solutions for antisymmetrically laminated anisotropic plates. J Appl Mech 1990;57:182–8.
[9] Noor AK, Burton WS. Assessment of shear deformation theories for multilayered composite plates. Appl Mech Rev 1989;42:1–13.
[10] Reddy JN. Energy and variational methods in applied mechanics. New York: Wiley, 1984.
[11] Reddy JN, Robbins Jr DH. Theories and computational models for composite laminates. Appl Mech Rev 1994;47:147–69.